

# Curing kinetics of self-healing epoxy thermosets

Manorama Tripathi · Devendra Kumar ·  
Chitra Rajagopal · Prasun Kumar Roy

Received: 2 April 2014 / Accepted: 23 August 2014 / Published online: 12 September 2014  
© Akadémiai Kiadó, Budapest, Hungary 2014

**Abstract** The curing kinetics of self-healing epoxy compositions was investigated by non-isothermal differential scanning calorimetric (DSC) studies. Cycloaliphatic epoxy resin was encapsulated in urea–formaldehyde (UF) using emulsion polymerisation technique to prepare epoxy-loaded UF microcapsules. Triethylene tetramine (TETA) hardener was immobilised on a mesoporous siliceous substrate (SBA 15) and both these additives were dispersed into an epoxy resin, which was subsequently cured using TETA. DSC studies revealed the autocatalytic nature of epoxy curing, which remained unaltered due to addition of the above-mentioned fillers, responsible for introducing self-healing functionality. The kinetic parameters of the curing process were determined using both Friedman and Kissinger–Akahira–Sunose (KAS) method. The activation energy at different degrees of conversion ( $E_{\alpha}$ ) was found to decrease with increasing degree of cure ( $\alpha$ ). Although UF resins possess secondary amine functionalities, which have the potential to react with the epoxy groups, no significant differences in the curing kinetics of the base resin were observed. Kinetic parameters were used to predict the curing behaviour of compositions at higher heating rates using KAS method. As expected, the onset curing temperature ( $T_{\text{onset}}$ ) and peak exotherm temperature ( $T_p$ ) of

epoxy shifted towards higher temperatures with increased heating rate; however, introduction of fillers does not affect these characteristic temperatures significantly. Also, the overall order of reaction does not vary significantly which supports the autocatalytic nature of curing reaction. The results suggests that although 2° amino groups are available with the UF resin, these do not directly participate in the curing reaction, as the primary amino groups in TETA are more easily accessible.

**Keywords** Curing kinetics · Autocatalytic reaction · Non-isothermal differential scanning calorimetry

## Introduction

The use of epoxy composites for structural applications has seen a tremendous increase in the last few decades, primarily because of their excellent thermo-mechanical, chemical and environmental stability. One of the major issues associated with these composites arises from the inherent brittleness of the epoxy matrix which renders these materials susceptible to microcrack formation. In the context of structural engineering, microcracking can prove to be rather fatal, as coalescence of microcracks can result in catastrophic failure of the components. An ideal route to increase the lifetime of components includes the usage of self-healing compositions, and in view of the same, such polymers have attracted increasing research interests lately [1–3]. At present, the most common strategy for imparting self-healing functionality involves introduction of fragile microcapsules, which encapsulate the healing agents [4]. During crack propagation, the embedded microcapsules rupture, leading to release of the healing agent into the

**Electronic supplementary material** The online version of this article (doi:10.1007/s10973-014-4128-1) contains supplementary material, which is available to authorized users.

M. Tripathi · C. Rajagopal · P. K. Roy (✉)  
Centre for Fire, Explosive and Environment Safety, Timarpur,  
Delhi 110054, India  
e-mail: pkroy@cfees.drdo.in; pk\_roy2000@yahoo.com

D. Kumar  
Department of Applied Chemistry and Polymer Technology,  
Delhi Technological University, Delhi 110042, India

crack plane and undergo polymerisation, which increases the overall lifetime of the polymer.

The choice of healing agents is practically unlimited; however, most common includes dicyclopentadiene and epoxy which undergo ring-opening polymerisation and curing reactions, respectively, in the presence of suitable catalysts, which too are embedded in the matrix. Different containment structures have been explored for encapsulating healing agents and in view of their reasonable cost and fragile nature, UF microcapsules are the most commonly used [5–7]. Nevertheless, the potential of hollow tubes [8, 9] and fibres has also been explored as healing agent containers. Unlike the hydrophobic epoxy-based healing resins, encapsulation of the curing agent, i.e. amine hardener, is relatively difficult and the procedure usually adopted involves preparation of hollow microcapsules into which the amines are vacuum infiltrated [10]. Alternatively, solid latent curing agents e.g.  $\text{CuBr}_2(2\text{-MeIm})_4$  have also been used, but the curing necessitates certain environmental conditions, particularly elevated temperatures, which may be difficult to be made available under field conditions [11].

We hypothesise that the amine hardener can easily be immobilised on mesoporous siliceous substrates e.g. SBA 15, MCM 41, etc. Lately, the scope of porous substrates towards immobilising enzymes has been explored extensively, [12–14] but surprisingly these have not yet been employed for loading amines. In this paper, we attempt to load a representative hardener, triethylene tetramine (TETA) on SBA 15 and investigate their effect on the curing behaviour of epoxy.

In view of the enormous potential of these self-healing materials in the future, it is very important to be cognizant of the effect of these self-healing additives on the curing kinetics, as this process governs the polymer morphology, which in turn, affects its properties [15–17]. A majority of studies in this area deal with improving the efficiency of self-healing process, but surprisingly very few studies deal with the kinetics of the curing process of such compositions [11, 18]. Of particular importance is to establish the role of common encapsulating materials e.g. UF which possess 2° amino functionalities capable of reacting with epoxy resins. In fact, UF resin has also been used as an effective hardener for epoxy resins, nonetheless the curing can be effected only at higher loadings (100 phr) [19]. Moreover, the silica nanoparticles have also been reported to alter the curing kinetics of epoxy, [20] and in view of the siliceous nature of SBA-15, its contribution towards altering the curing behaviour of epoxy needs to be studied.

The aim of the present work is to study the effect of self-healing fillers on the curing kinetics of a cycloaliphatic epoxy resin with TETA hardener. For this purpose, non-isothermal DSC measurements have been carried out and

empirical approaches are used to model the kinetics of the curing reactions.

## Experimental

### Materials

Urea, formalin (37 % formaldehyde in water), citric acid, polyvinyl alcohol (PVA) (Mw 14,000) (CDH) and triethanol amine (Merck) were used without any further purification. Tetraethyl orthosilicate (TEOS) and P-123 amphiphilic block-copolymer poly (ethylene oxide)-poly (propylene oxide)-poly (ethylene oxide), ( $\text{EO}_{20}\text{PO}_{70}\text{EO}_{20}$ ) were purchased from Aldrich and used as silica precursor and the organic template, respectively. An amine-cured epoxy resin (Ciba Geigy, Araldite CY 230; epoxy equivalent 200 eq  $\text{g}^{-1}$ ) and TETA hardener (HY 951; amine content 32 eq  $\text{kg}^{-1}$ ) were used as received. Distilled water was used throughout the course of study.

### Preparation of microcapsules

The preparation of epoxy-encapsulated UF microcapsules by oil-in-water (O/W) emulsion polymerisation route has been described in our previous paper [21]. In brief, urea (5 g) and formalin (10 g) were dissolved in distilled water (35 mL) under continuous stirring at room temperature. The pH of resulting solution was slowly increased to 8–9 by dropwise addition of triethanolamine, while maintaining the temperature at  $343 \pm 5$  K for 1 h to obtain a prepolymer solution [22]. The solution was cooled and to this was added an aqueous solution of PVA (2.5 mL, 5 % w/w), which was followed by the addition of a slow stream ( $0.5 \text{ mL min}^{-1}$ ) of epoxy resin to form an emulsion. Post stabilisation, the pH of the emulsion was brought down to 3–4 by addition of requisite amount of aqueous citric acid solution (5 % w/v), while increasing the temperature of the solution at a rate of  $1 \text{ Kmin}^{-1}$  to  $323 \pm 2$  K. After 3 h, the obtained suspension of microcapsules was cooled down to ambient temperature, filtered, washed repeatedly with distilled water and acetone and air-dried for 24 h.

The extent of encapsulation in the microcapsules was determined by acetone extraction method as per the reported procedure [7]. For this purpose, an accurately weighed amount of microcapsules ( $M_{\text{mc}}$ ) was crushed to release the encapsulated epoxy resin. The resulting powder was then repeatedly washed with acetone to extract the epoxy, filtered, dried and weighed ( $M_{\text{shell}}$ ). The core content was determined gravimetrically as the ratio of encapsulated mass of epoxy to the total mass of the microcapsules.

$$\text{Core content} = \frac{M_{\text{mc}} - M_{\text{shell}}}{M_{\text{mc}}} \quad (1)$$

#### Assembly of mesoporous SBA-15

The preparation of SBA 15 using a polymer-templated technique has been reported in our previous paper [23]. In brief, 1.22 g of the amphiphilic block-copolymer was dissolved in 715 mL of water and 110 mL of 16 M HCl under stirring at  $318 \pm 1$  K for 16 h. 50 mL of TEOS was introduced to this solution, and the hydrolysis was allowed to proceed for 8 h under stirring. The product obtained was washed with water and dried at 383 K prior to calcination at a controlled heating rate of  $1 \text{ K min}^{-1}$  up to 873 K.

#### Hardener immobilisation on SBA-15

Amine was entrapped in the pores of the mesoporous silica by physical adsorption technique. The immobilisation was achieved by placing 10 g of SBA-15 in excess of free amine and incubating the mixture at 298 K under shaking (150 rpm). After 24 h incubation, the sample was subjected to centrifugation at 600 rpm for 5 min and washed with copious amounts of ethanol. The increase in mass was used to quantify the extent of amine loading

$$\text{Immobilised amine (mg mg}^{-1}\text{)} = \frac{E_f - E_o}{E_o} \quad (2)$$

where  $E_f$  is the mass of amine immobilised SBA 15 and  $E_o$  is the mass of SBA 15 taken for immobilisation.

#### Characterisation methods

The surface morphology of samples was studied using a scanning electron microscope (Zeiss EVO MA15) under an acceleration voltage of 20 kV. Samples were mounted on aluminium stubs and sputter coated with gold and palladium (10 nm) using a sputter coater (Quorum-SC7620) operating at 10–12 mA for 120 s. The textural property of SBA 15 was determined by  $\text{N}_2$  adsorption–desorption on a Surface Area Analyser (Micromeritics ASAP 2010). The identification of crystalline phases in the sample was performed by powder XRD analysis on a Philips PANalytical 1730 diffractometer using  $\text{Cu K}\alpha$  ( $\lambda = 1.54 \text{ \AA}$ ), where the diffractograms were recorded over a range of  $2\theta = 0^\circ$ – $10^\circ$ . The pore wall thickness was calculated as  $d(100) \cdot 2/\sqrt{3}$ —pore diameter, where  $d(100)$  is the d-spacing value of the (100) diffraction peak in XRD patterns of the silica sample [24].

Fourier transform infrared spectra of samples were recorded in the wavelength range of  $4,000$ – $600 \text{ cm}^{-1}$  using FTIR spectroscopy on a Thermo Fisher FTIR (NICOLET 8700) analyser with an attenuated total reflectance (ATR)

crystal accessory. Calorimetric studies were performed on a Differential Scanning Calorimeter (TA instruments Q20). The resin and TETA were mixed at a stoichiometric epoxide/amine ratio (100:13) at low temperatures (0–5 K). For dynamic DSC scans, samples ( $10 \pm 2 \text{ mg}$ ) were sealed in aluminium pans and heated from 273 to 523 K at four different rates 2.5, 5, 10 and  $15 \text{ K min}^{-1}$ . Nitrogen was purged at rate of  $50 \text{ mL min}^{-1}$  to minimise oxidation of the sample during the curing process. Isothermal runs were performed on selected samples at 313 K for 1 h. Prior to the experiments, the instrument was calibrated for temperature and enthalpy using standard indium and zinc. Thermal equilibrium was regained within 1 min of sample insertion, and the exothermic reaction was considered to be complete when the recorder signal levelled off to the baseline. The total area under the exothermic curve was determined to quantify the heat of curing. The thermogravimetric analysis was performed on a Perkin Elmer simultaneous TG/DTA instrument (Diamond SDTA), for which the samples were heated from 323 to 873 K, under air atmosphere at a programmed heating rate of  $10 \text{ K min}^{-1}$ . The amount of microcapsule loading in epoxy was selected based on reported previous studies, [6] and the amount of loaded SBA-15 was decided on the basis of stoichiometric requirements. The samples have been designated as EP followed by the concentration of UF microcapsules (% w/w) and concentration of mesoporous silica. E.g. epoxy containing 10 % UF microcapsules and 2 % mesoporous silica will be referred to as EP10UF2MS and neat epoxy will be referred to as EP throughout the text.

## Results and discussion

Epoxy-encapsulated UF microcapsules were prepared by oil-in-water emulsion technique, and TETA hardener (HY 951) was immobilised within the pores of mesoporous silica (SBA 15). Self-healing epoxy composites were prepared by dispersing known amount of the microcapsules and immobilised amine hardener in epoxy resin and the curing behaviour of the compositions was studied by non-isothermal calorimetry to gain insight into the effect of self-healing fillers on the curing kinetics of epoxy resin.

#### Epoxy-encapsulated urea–formaldehyde microcapsules

The SEM image of a representative batch of epoxy-encapsulated UF microcapsules is presented in Fig. 1. It can be seen that the microcapsules are spherical in shape, with a rough surface texture, a feature which could be attributed to the presence of protruding polymer nanoparticles [25]. The interior of the microcapsule is, however,

smooth and the thickness of the shell wall, as determined from the SEM images, was found to be  $\sim 350 \pm 54$  nm (Supplementary information, Figure S1). It is to be noted that the microcapsule size could be controlled by varying the rate of agitation during the polymerisation process. In the present study, a stirring speed of 250 rpm was employed, which yielded microspheres of dimensions satisfactory for the use in self-healing application [25], i.e. (diameter  $\sim 190 \pm 49$   $\mu\text{m}$ ). The core content of the microcapsules was determined to be  $65 \pm 5$  %, which could be attributed to the presence of UF debris.

Fourier transform infrared spectra of urea–formaldehyde microcapsules are presented in Fig. 2. Urea–formaldehyde microcapsules exhibit characteristic broadband around  $3,301\text{ cm}^{-1}$  which arises from the overlapping absorptions due to hydroxyl, imino and amino functionalities. Other characteristic absorptions include alkyl C–H stretching ( $2,962\text{ cm}^{-1}$ ), C–H bending ( $1,383\text{ cm}^{-1}$ ), aliphatic C–N

( $1,242$  and  $1,182\text{ cm}^{-1}$ ), NH–CO–NH stretching ( $1,649\text{ cm}^{-1}$ ) and C–O–C stretching ( $1,032\text{ cm}^{-1}$ ) [26].

TG trace of epoxy-encapsulated UF is presented in Fig. 3. The initial mass loss of  $\sim 3.6$  % ( $T < 423$  K) can be attributed to the removal of water (DSC trace, Figure S2), and the subsequent loss corresponds to the removal of methanol and formaldehyde. Further heating leads to the transformation of methylene ether bridges into methylene bridges at  $\sim 473$  K, a phenomenon associated with loss of formaldehyde. The subsequent mass loss at  $573$ – $663$  K occurs due to pyrolytic degradation of the resultant cross-linked network.

#### Immobilisation of amine hardener

Detailed characterisation of the mesoporous siliceous substrate prepared by the polymer-templated route is discussed elsewhere [27]. The mesoporous nature of SBA 15

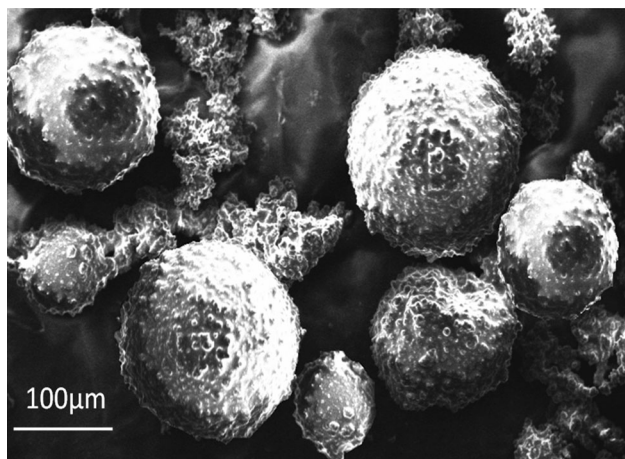


**Fig. 1** SEM images of epoxy-encapsulated urea–formaldehyde microcapsules

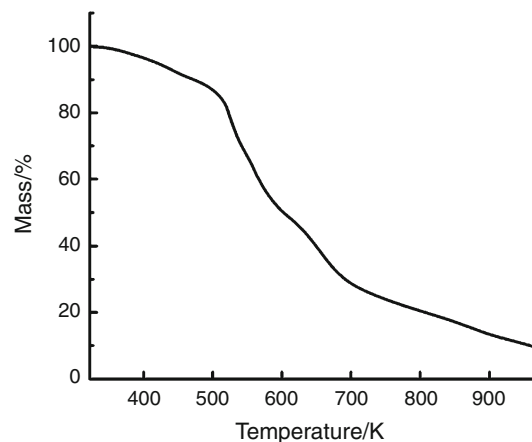


**Fig. 3** TG trace of epoxy-encapsulated urea–formaldehyde microcapsules

**Fig. 2** FTIR spectrum of epoxy-encapsulated urea–formaldehyde microcapsules

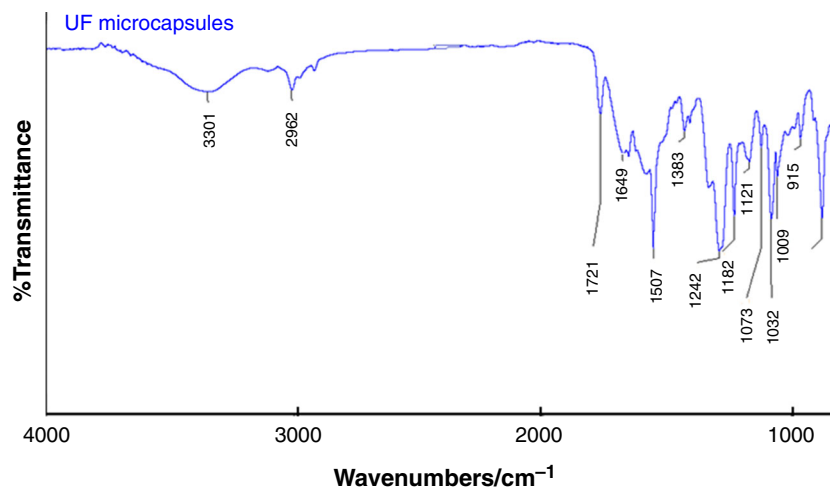
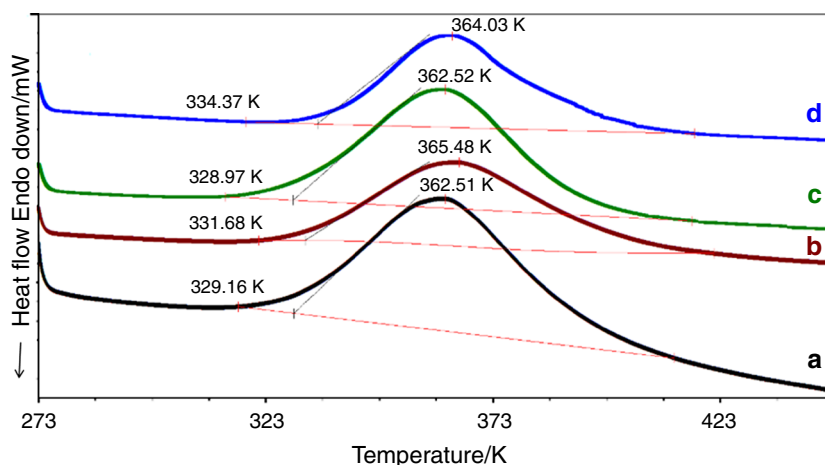


**Fig. 4** Curing profile of epoxy-based compositions *a* Neat epoxy, *b* EP5UF, *c* EP10UF, *d* EP10UF2MS



was confirmed by a type II hysteresis loop evidenced in  $N_2$  adsorption–desorption isotherm. The BET surface area was found to be  $808 \text{ m}^2 \text{ g}^{-1}$  and a uniform average pore diameter of 5.4 nm was determined by the Barrett–Joyner–Halenda (BJH) method which was applied on the desorption branch of the isotherm. The XRD of SBA 15 is presented in the supplementary section (Figure S3), which was used to estimate the  $d(100)$  value of 8.84 nm and wall thickness of 4.8 nm, which match well with the values reported in the literature [24].

In view of the simplicity of the method, physical adsorption technique was used for immobilising the TETA hardener. The extent of loading was found to be  $5 \text{ mg mg}^{-1}$  as established from gravimetric studies. Chemical interactions between the siliceous substrate and the amine, particularly hydrogen bonding and acid–base interactions can be held responsible for the high loading values.

#### Curing behaviour

The DSC traces of neat epoxy and microcapsule filled compositions under a representative heating rate ( $5 \text{ K min}^{-1}$ ) are presented in Fig. 4. It is apparent from the figure that all the compositions exhibit a single exothermic peak, which is characteristic of the epoxy curing process. The presence of UF microcapsules or amine immobilised SBA-15 did not seem to affect the curing process appreciably and all the compositions exhibit similar onset cure temperature ( $T_{\text{onset}}$ ) and peak cure temperature ( $T_{\text{peak}}$ ) values.

Differential scanning calorimetric curves of a representative epoxy composite at various heating rates viz. 2.5, 5, 10 and  $15 \text{ K min}^{-1}$  are presented in Fig. 5. As expected, increasing the heating rate ( $\beta$ ) leads to a systematic shift in the trace towards higher temperatures. The curing reaction is primarily a kinetic event, which is a function of both time and temperature. On being subjected to a higher heating rate, the reactants get lesser time to react at any specific temperature, leading to the observed phenomenon.

The characteristic thermal parameters i.e.  $\Delta H_{\text{cure}}$ ,  $T_{\text{onset}}$  and  $T_{\text{peak}}$  are summarised in Table 1.

It is apparent from the data that there is no significant effect on the heat of curing ( $\Delta H_{\text{cure}}$ ) due to increasing heating rates. The extent of conversion ( $\alpha$ ) at any particular temperature ( $T_x$ ) was estimated as the ratio of the areas under the exothermic DSC peak:

$$\alpha = \frac{\Delta H_{T_x}}{\Delta H_{\text{cure}}}, \quad (3)$$

where  $\Delta H_{T_x}$  is the heat of reaction of partially cured samples (till temperature  $T_x$ ) and  $\Delta H_{\text{cure}}$  is the total heat of reaction.

The increase in the degree of conversion with temperature for EP, and EP5UF, EP10UF and EP10UF2MS at a particular heating rate ( $5 \text{ K min}^{-1}$ ) is presented in Fig. 6. It can be seen that microcapsule loading does not lead to any significant effect on the curing behaviour as far as the degree of conversion is concerned. As expected [28], the trace shifts towards higher temperature with increasing heating rate, as is apparent from the data presented in Fig. 7.

#### Isoconversion methods

The rate of a reaction is primarily dependent on three major variables: temperature ( $T$ ), extent of conversion ( $\alpha$ ) and pressure ( $P$ ) as follows:

$$\frac{d\alpha}{dt} = k(T)f(\alpha)h(P) \quad (4)$$

The pressure term, ( $h(P)$ ), is generally ignored for a majority of kinetics methods, and the reaction rate can be rewritten as

$$\frac{d\alpha}{dt} = k(T)f(\alpha) \quad (5)$$

Generally, the temperature-dependent term ( $k(T)$ ) is assumed to exhibit Arrhenius type dependency



**Fig. 5** Effect of heating rate on the DSC traces of microcapsule filled epoxy (EP5UF) *a* 2.5, *b* 5, *c* 10 and *d* 15 K min<sup>-1</sup>

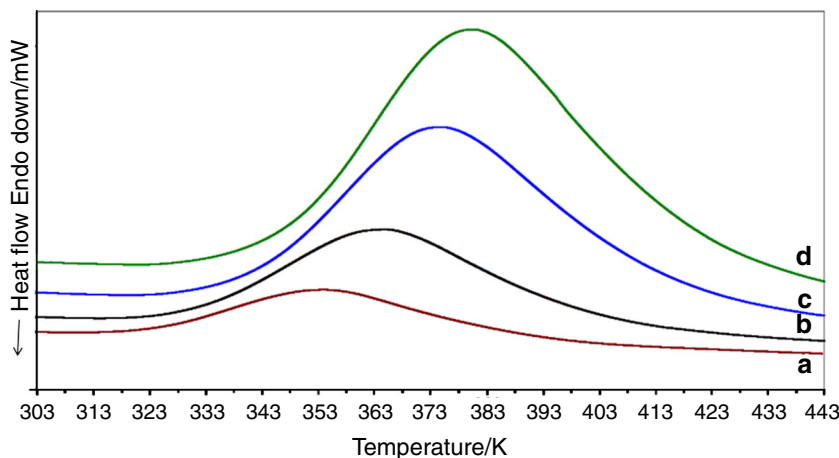


**Table 1** Characteristic curing parameters of epoxy and self-healing compositions

Sample	$\beta/\text{K min}^{-1}$	$T_{\text{onset}}/\text{K}$	$T_{\text{peak}}/\text{K}$	$\Delta H_{\text{cure}}/\text{J g}^{-1}$
Epoxy	2.5	327.1	352.2	320.3
	5	329.2	362.5	323.5
	10	338.3	375.3	342.8
	15	348.3	380.0	321.7
EP5UF	2.5	322.9	354.6	305.6
	5	331.7	365.5	311.3
	10	340.2	375.4	309.4
EP10UF	15	345.5	381.1	294.3
	2.5	321.6	353.3	319.5
	5	328.9	362.5	328.2
EP10UF2MS	10	339.3	377.9	327.8
	15	355.7	385.1	321.6
	2.5	329.4	354.4	300.5
	5	334.4	364.0	310.2
	10	342.2	374.3	312.8
	15	347.3	374.8	307.6

$$k(T) = A \exp\left(-\frac{E}{RT}\right) \quad (6)$$

Combining Eqs. 5 and 6

$$\frac{d\alpha}{dt} = A \exp\left(-\frac{E_{\alpha}}{RT}\right) f(\alpha) \quad (7)$$

where  $f(\alpha)$  is the reaction model,  $T$  (K) is the absolute temperature,  $A$  (s<sup>-1</sup>) is the pre-exponential factor,  $E_{\alpha}$  (kJ mol<sup>-1</sup>) is the activation energy and  $R$  the universal gas constant. For different heating rates ( $\beta_i$ ), Friedman method directly gives Eq. 8 at specified  $\alpha$

$$\ln\left(\frac{d\alpha}{dt}\right)_{\alpha_i} = \ln(A_{\alpha} f(\alpha)) - \frac{E_{\alpha}}{RT_{\alpha_i}} \quad (8)$$

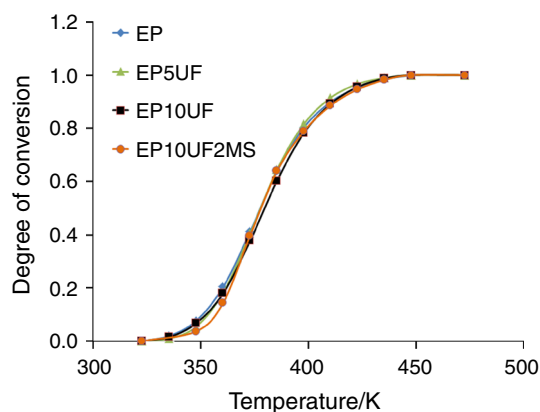


**Fig. 6** Effect of temperature on the degree of conversion of epoxy and self-healing composition ( $\beta = 5 \text{ K min}^{-1}$ )

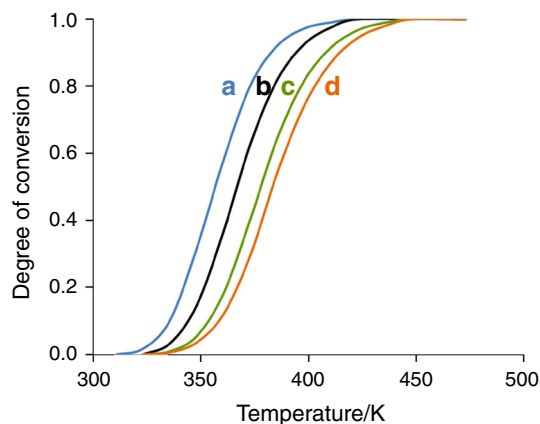


**Fig. 7** Effect of temperature and heating rate on the extent of epoxy curing *a* 2.5, *b* 5, *c* 10 and *d* 15 K min<sup>-1</sup>

By substituting a new parameter  $C_f(\alpha) = \ln(A_{\alpha} f(\alpha))$ , Eq. 8 may be written as

$$\ln\left(\frac{d\alpha}{dt}\right)_{\alpha_i} = C_f(\alpha) - \frac{E_{\alpha}}{RT_{\alpha_i}} \quad (9)$$

At a particular conversion ( $\alpha$ ), parameters  $\left(\frac{d\alpha}{dt}\right)_{\alpha_i}$  and  $T_{\alpha,i}$  values can be determined experimentally at different heating rates. This can be used to arrive at  $E_{\alpha}$  and  $C_f(\alpha)$  from the plot of  $\ln\left(\frac{d\alpha}{dt}\right)_{\alpha_i}$  versus  $\frac{1}{T_{\alpha,i}}$  for at least three heating rates.

Alternatively, Kissinger–Akahira–Sunose method can be used for determination of activation energy ( $E_{\alpha}$ ) [29]. For this method,  $\left(\frac{d\alpha}{dt}\right)$  can be equated to  $\frac{d(\alpha)}{dT}\beta$ , and Eq. 7 can be further rearranged.

$$\frac{d\alpha}{f(\alpha)} = \frac{A}{\beta} \exp\left(-\frac{E_{\alpha}}{RT}\right) dT \quad (10)$$

Integrating Eq. 10 and introducing Doyle's approximation [30] lead to

$$g(\alpha) = \int_0^{\alpha} \frac{d(\alpha)}{f(\alpha)} = \frac{A}{\beta} \int_{T_0}^T \exp\left(-\frac{E}{RT}\right) dT \cong \frac{ART^2}{\beta E} \exp\left(-\frac{E}{RT}\right) \quad (11)$$

By taking logarithm of Eq. 11, the following equation can be derived for various heating rates under a constant degree of conversion  $\alpha$ ,

$$\ln\left(\frac{\beta}{T_{\alpha,i}^2}\right) = \ln\left(\frac{RA_{\alpha}}{E_{\alpha}g(\alpha)}\right) - \frac{E_{\alpha}}{RT_{\alpha,i}} \quad (12)$$

which can further be written as

$$\ln\left(\frac{\beta}{T_{\alpha,i}^2}\right) = C_k - \frac{E_{\alpha}}{RT_{\alpha,i}}, \quad (13)$$

where  $C_k(\alpha) = \ln\left(\frac{RA_{\alpha}}{E_{\alpha}g(\alpha)}\right)$

Hence,  $E_{\alpha}$  can be obtained using the KAS method from the slope of  $\ln\left(\frac{\beta}{T_{\alpha,i}^2}\right)$  against  $\frac{1}{T_{\alpha,i}}$ .

The linear plots (at selected conversions) used to arrive at the activation energy using KAS and Friedman method for EP5UF are depicted in the supplementary section

(Figure S4). The variation of activation energy as a function of degree of conversion ( $\alpha$ ) for neat epoxy and the self-healing compositions, as determined by both the methods is presented in Fig. 8. It can be seen that the range of activation energies for all the composition is between 40 and 90 kJ mol<sup>-1</sup>, irrespective of the model employed. In general, a progressive decrease in the activation energies was observed. It was interesting to note that the introduction of UF fillers or amine loaded SBA15 does not affect the activation energy-conversion profile. The reaction of the epoxy groups with amine leads to formation of a solid polymer [31], which is expected to switch the kinetically controlled process to one that of diffusion controlled, thereby expected to lead to an increase in the  $E_{\alpha}$ . However, the exothermic curing process results in an increase in the energy of the reactants, indirectly lowering the energy required to cross the energy barrier. In view of the higher reactivity of the 1° amine groups with epoxy, this reaction predominates in the early stages of curing ( $\alpha < 0.6$ ). This is followed by the reaction with 2° amines, which continues until  $\alpha = 0.8$  [32]. Towards the end of the cure process, i.e. at higher temperatures, other reactions such as etherification and homopolymerisation of epoxide groups have also been reported. It is the combined result of all of the above processes which manifests in the observed  $E_{\alpha} - \alpha$  profile. Interestingly, the curing of epoxy has been effected by UF at higher loadings (50:50) [19]; however, our results suggests that although 2° amino groups are available on the surface of UF resin, these do not directly participate in the curing reaction, as the primary amino groups in the liquid TETA are more easily accessible.

#### Prediction of dynamic cure of self-healing epoxy resin

In view of its simplicity, KAS method was used to predict the curing behaviour of self-healing epoxy composites, when cured under different heating rates. For this purpose,

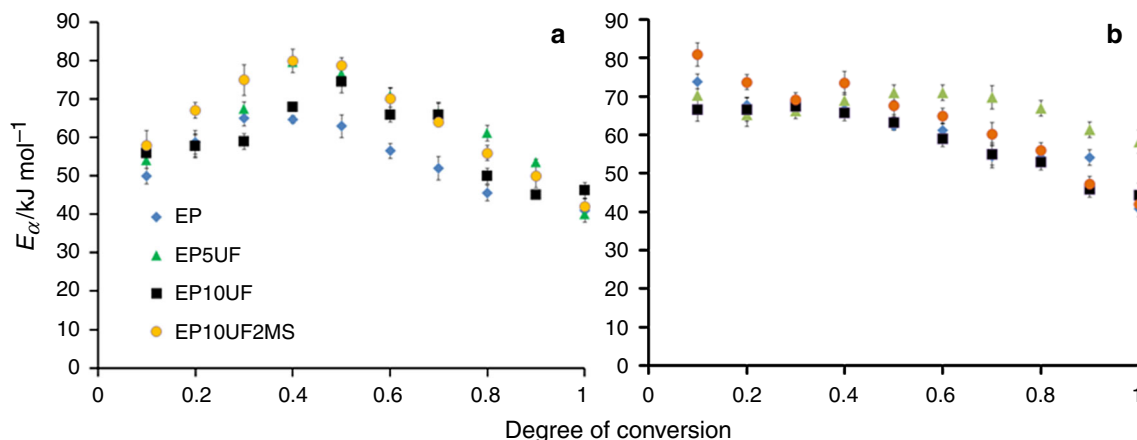


**Fig. 8** Variation of activation energy ( $E_{\alpha}$ ) with extent of conversion **a** Friedman method **b** Kissinger–Akahira–Sunose method

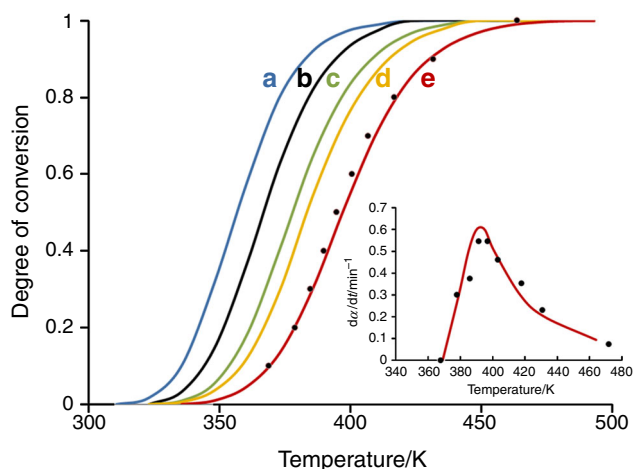


**Fig. 9** Experimentally determined curing degree at different heating rates (a) 2.5, (b) 5, (c) 10, (d) 15 and (e) 30 K min<sup>-1</sup>. Inset shows the experimental and KAS predicted reaction rate at 30 K min<sup>-1</sup>

$C_k(\alpha)$  and  $E_\alpha$  derived from the data obtained at  $\beta = 2.5, 5, 10$  and  $15$  K min<sup>-1</sup> were substituted into Eq. 13 to quantify the temperature associated with different values of  $\alpha$  under a particular heating rate ( $\beta$ ). The model was further validated by performing dynamic DSC run at 30 K min<sup>-1</sup>, and the experimental values are presented in Fig. 9. The variation of rate of reaction ( $\frac{d\alpha}{dt}$ ) as a function of temperature for the specified heating rate (30 K min<sup>-1</sup>) is presented in the inset of Fig. 9. It can be seen that the predicted values are in close agreement with the data obtained experimentally.

To establish the potential of the proposed self-healing system comprising of epoxy-encapsulated UF microcapsules and amine immobilised on SBA 15, curing was also effected on a mixture containing stoichiometric amounts of crushed microcapsules and SBA 15. The resulting calorimetric trace is presented in the supplementary section (Figure S5). The curve exhibits a single exothermic peak, characteristic of curing process associated with the epoxy released from the microcapsules with the hardener. However, the heat of curing ( $\Delta H_{\text{cure}}$ ) was found to be 170.2 J g<sup>-1</sup> as compared to 342.8 J g<sup>-1</sup> for neat epoxy under similar experimental conditions (10 K min<sup>-1</sup>), which relates well with the core content of the microcapsules.

## Conclusions

The curing behaviour of a cycloaliphatic epoxy cured with triethylene tetramine hardener and representative self-healing compositions prepared by dispersing UF microcapsules and SBA 15 immobilised amine has been systematically studied using the non-isothermal DSC

technique. Curing studies were performed at different heating rates (2.5–15 K min<sup>-1</sup>) and the data were used to determine the activation energy at different stages of curing, using both Friedman and Kissinger–Akahira–Sunose methods. The activation energies were found to vary from 40 to 90 kJ mol<sup>-1</sup> irrespective of the method being used for estimation. The studies revealed a progressive decrease in the activation energy for all compositions, irrespective of the presence of microcapsules or SBA 15 in the composition in the concentration range studied. KAS method was further used to predict the curing behaviour at elevated heating rate 30 K min<sup>-1</sup>, which was subsequently validated with dynamic DSC experiments.

## References

1. Yang Y, Urban MW. Self-healing polymeric materials. *Chem Soc Rev.* 2013;42(17):7446–67.
2. Scheltjens G, Brancart J, Graeve I, Mele B, Terryn H, Assche G. Self-healing property characterization of reversible thermoset coatings. *J Therm Anal Calorim.* 2011;105(3):805–9.
3. Sharma P, Shukla S, Lochab B, Kumar D, Roy PK. Microencapsulated cardanol derived benzoxazines for self-healing applications. *Mater Lett.* 2014;. doi:10.1016/j.matlet.2014.07.048.
4. White SR, Sottos NR, Geubelle PH, Moore JS, Kessler MR, Sriram SR, et al. Autonomic healing of polymer composites. *Nature.* 2001;409(6822):794–7.
5. Kessler MR, Sottos NR, White SR. Self-healing structural composite materials. *Compos A.* 2003;34(8):743–53.
6. Brown EN, White SR, Sottos NR. Microcapsule induced toughening in a self-healing polymer composite. *J Mater Sci.* 2004;39(5):1703–10.
7. Yuan L. Preparation and characterization of poly(urea-formaldehyde) microcapsules filled with epoxy resins. *Polym Degrad Stab.* 2006;47:5338–49.
8. Bleay SM, Loader CB, Hawyes VJ, Humberstone L, Curtis PT. A smart repair system for polymer matrix composites. *Compos A Appl Sci Manuf.* 2001;32(12):1767–76.
9. Pang JWC, Bond IP. A hollow fibre reinforced polymer composite encompassing self-healing and enhanced damage visibility. *Compos Sci Technol.* 2005;65(11–12):1791–9.
10. Jin H, Mangun CL, Stradley DS, Moore JS, Sottos NR, White SR. Self-healing thermoset using encapsulated epoxy-amine healing chemistry. *Polymer.* 2012;53(2):581–7.
11. Yin T, Rong M, Zhang LM. Self-healing epoxy composites—part I: curing kinetics and heat-resistant performance. *Adv Mater Res.* 2013;716:383–6.
12. Hudson S, Magner E, Cooney J, Hodnett BK. Methodology for the immobilization of enzymes onto mesoporous materials. *J Phys Chem B.* 2005;109(41):19496–506.
13. Karimi B, Emadi S, Safari AA, Kermanian M. Immobilization, stability and enzymatic activity of albumin and trypsin adsorbed onto nanostructured mesoporous SBA-15 with compatible pore sizes. *RSC Adv.* 2014;4:4387–4394.
14. Yiu HHP, Wright PA, Botting NP. Enzyme immobilisation using SBA-15 mesoporous molecular sieves with functionalised surfaces. *J Mol Catal B Enzym.* 2001;15(1–3):81–92.
15. Chaudhary S, Parthasarathy S, Kumar D, Rajagopal C, Roy PK. Graft-interpenetrating polymer networks of epoxy with polyurethanes derived from poly(ethyleneterephthalate) waste. *J Appl Polym Sci.* 2014;131:40490.



16. Chaudhary S, Parthasarathy S, Kumar D, Rajagopal C, Roy PK. Poly(ethyleneterephthalate) glycolysates as effective toughening agents for epoxy resin. *J Appl Polym Sci*. 2014;131:39941.
17. Ramírez C, Abad MJ, Barral L, Cano J, Díez FJ, López J, et al. Thermal behaviour of a polyhedral oligomeric silsesquioxane with epoxy resin cured by diamines. *J Therm Anal Calorim*. 2003;72(2):421–9.
18. Tong XM, Zhang M, Yang MZ. Study on the curing kinetics of epoxy resin in self-healing microcapsules with different shell material. *Adv Mater Res*. 2011;306–307:658–62.
19. Ghaemy M, Yaghoob S, Karimi M. Curing kinetics of DGEBA/UF resin system used as laminates in impregnated decorative paper. *Iran Polym J*. 2010;19(9):661–8.
20. Rosso P, Ye L. Epoxy/Silica nanocomposites: nanoparticle-induced cure kinetics and microstructure. *Macromol Rapid Commun*. 2007;28(1):121–6.
21. Tripathi M, Rahamtullah, Kumar D, Rajagopal C, Roy PK. Influence of microcapsule shell material on the mechanical behavior of epoxy composites for self-healing applications. *J Appl Polym Sci*. 2014;131:40572.
22. Yuan YC, Rong MZ, Zhang MQ, Chen J, Yang GC, Li XM. Self-healing polymeric materials using epoxy/mercaptan as the healant. *Macromolecules*. 2008;41(14):5197–202.
23. Meynen V, Cool P, Vansant EF. Verified syntheses of mesoporous materials. *Microporous Mesoporous Mater*. 2009;125(3):170–223.
24. Naskar MK, Eswaremoorthy M. Significant improvement in the pore properties of SBA-15 brought about by carboxylic acids and hydrothermal treatment. *J Chem Sci*. 2008;120(1):181–6.
25. Brown EN. In situ poly(urea-formaldehyde) microencapsulation of dicyclopentadiene. *J Microencapsul*. 2003;20(6):719–30.
26. Salaün F, Vroman I. Influence of core materials on thermal properties of melamine–formaldehyde microcapsules. *Eur Polym J*. 2008;44(3):849–60.
27. Roy PK, Ullas AV, Chaudhary S, Mangla V, Sharma P, Kumar D, et al. Effect of SBA-15 on the energy absorption characteristics of epoxy resin for blast mitigation applications. *Iran Polym J*. 2013;22(9):709–19.
28. Wang J, Laborie M-PG, Wolcott MP. Comparison of model-free kinetic methods for modeling the cure kinetics of commercial phenol–formaldehyde resins. *Thermochim Acta*. 2005;439(1–2):68–73.
29. Budrugaec P, Segal E. Applicability of the Kissinger equation in thermal analysis. *J Therm Anal Calorim*. 2007;88(3):703–7.
30. Doyle CD. Kinetic analysis of thermogravimetric data. *J Appl Polym Sci*. 1961;5(15):285–92.
31. Ghumara R, Adroja P, Parsania PH. Synthesis, characterization, and dynamic DSC curing kinetics of novel epoxy resin of 2,4,6-tris(4-hydroxyphenyl)-1-3-5-triazine. *J Therm Anal Calorim*. 2013;114(2):873–81.
32. Prime RB. Thermal characterization of polymeric materials. New York: Academic; 1997.